We are IntechOpen, the world's leading publisher of Open Access books Built by scientists, for scientists

4,800
Open access books available

122,000
International authors and editors

135M
Downloads

Our authors are among the

154
Countries delivered to

TOP 1%
most cited scientists

12.2%
Contributors from top 500 universities

CLARIVATE ANALYTICS
BOOK CITATION INDEX
INDEXED

WEB OF SCIENCE™

Selection of our books indexed in the Book Citation Index
in Web of Science™ Core Collection (BKCI)

Interested in publishing with us?
Contact book.department@intechopen.com

Simulation Platform for Performance Analysis of Cooperative Eigenvalue Spectrum Sensing with a Realistic Receiver Model Under Impulsive Noise

Rausley Adriano Amaral de Souza,

Dayan Adionel Guimarães and

André Antônio dos Anjos

Additional information is available at the end of the chapter

1. Introduction

Currently, the assignment of the electromagnetic spectrum for wireless communication systems follows the so-called fixed allocation policy. In this policy, those who are paying for a given portion of the spectrum obtain the license for exclusively use it, in spite of actually not occupying that portion during all time and in the entire coverage area. This fixed allocation policy, along with the large growth in wireless communications systems and services have led to spectrum congestion and underutilization at the same time [1]. With the advent of the cognitive radio (CR) paradigm [2], cognition-inspired dynamic spectrum access techniques come into action by exploring the underutilized portions of the spectrum in time and space, while causing no or minimum harm in the system that owns the license. In this context, the cognitive radio network is called secondary network, whereas the network licensed for using the spectrum is called primary network.

Among the enormous variety of cognitive tasks that a CR can perform, spectrum sensing is the task of detecting holes (whitespaces) in frequency bands licensed to primary wireless networks, for opportunistic use by the secondary network. Although sensing can be performed by each secondary receiver in a non-cooperative fashion, cooperative spectrum sensing, also known as collaborative spectrum sensing [3], has been considered a solution for problems experienced by CR networks in a non-cooperative sensing situation [4].

In this chapter we first review the main concepts related to the cooperative spectrum sensing, with focus on recent techniques based on the eigenvalues of the received signal covariance matrix, namely: the eigenvalue-based generalized likelihood ratio test (GLRT), the maximum-minimum eigenvalue detection (MMED), the maximum eigenvalue detection (MED), and the energy detection (ED). Then we localize the spectrum sensing subject in the context of vehicular networks. Each cognitive radio is modeled according to a real CR receiver architecture and the sensing environment model considers not only channel fading and thermal noise, but also the presence of impulsive noise (IN). We then describe a MATLAB[1]-based simulation platform developed under the above models, aimed at assessing the performance of several spectrum sensing techniques.

2. Spectrum sensing fundamentals

Figure 1 illustrates a spectrum sensing scenario with a secondary cognitive radio network sharing the spectrum licensed to a primary TV broadcast network, a typical situation covered by the recently issued IEEE 802.22 Standard [5]. In this figure, the coverage areas of the primary transmitters PT1 and PT2 are reaching the cognitive radios CR1 and CR2. Thus, both CRs can check if these primary transmitters are active in a given band (channel) and, if not, the secondary network can opportunistically use that spectrum band. At regular time intervals, the CRs must interrupt their transmissions and verify if the channel is still unoccupied by the primary network. If the channel becomes occupied, the secondary network must stop their transmissions and start the search for another vacant channel.

The decision upon the spectrum occupancy can be independently (non-cooperatively) made by each CR or can be reached by means of cooperation among multiple CRs. In the first case, the sensing performance can be drastically affected by the channel between PTs and CRs. As an example, suppose that a given CR is in a deep fading situation or in a shadowed coverage area, like a topographic depression, inside a building with high radio penetration loss, a tunnel, or behind a large building. This CR can erroneously decide that a channel is vacant and start to use it, causing a harmful interference in the primary network. A similar situation occurs if a CR is out of the reach of the primary network coverage, which is the case of CR3 in Figure 1. It can decide that the sensed channel is vacant, causing strong interference in nearby primary terminals (in T3 in this example). On the other hand, in cooperative spectrum sensing multiple CRs can benefit from the spatial diversity and reduce the effect of the abovementioned problems. Under the control of a secondary base station (BS), a number of CRs monitor a given channel and the decision upon the channel occupancy is made based on the information from all cooperating CRs.

Cooperative spectrum sensing can be classified as centralized and distributed, with the possibility of being relay-assisted [6] in both situations, as illustrated in Figure 2.

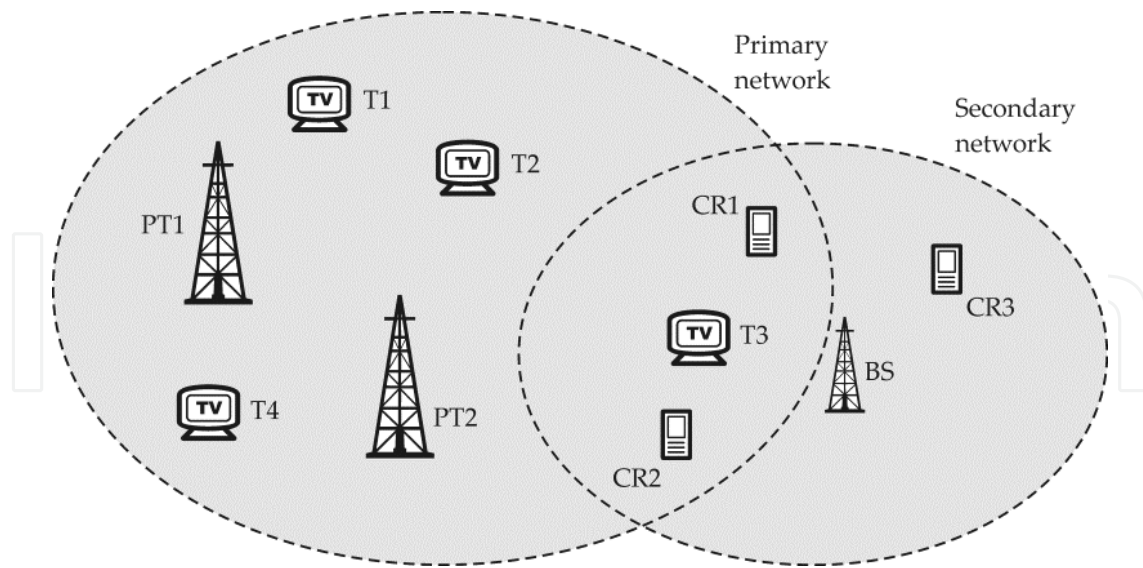1 Matlab is a commercial produt sold by The mathworks, Inc,

Figure 1. A secondary cognitive radio network opportunistically using the spectrum licensed to a primary TV broadcast network.
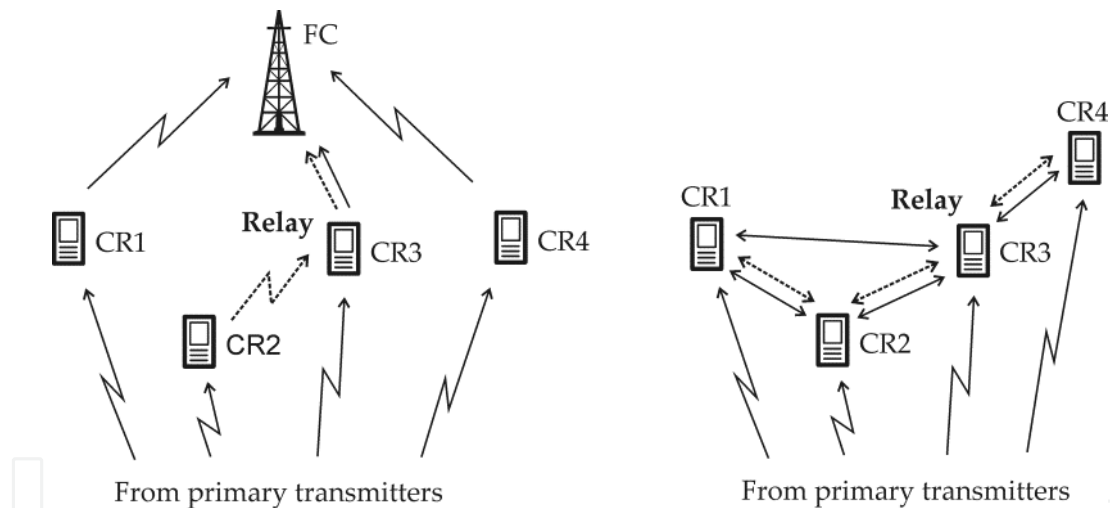

Figure 2. Classification of cooperative spectrum sensing (left) centralized, (right) distributed.

In centralized cooperative sensing, data collected by each cooperating CR (e.g., received samples) are sent via a reporting control channel to a fusion center (FC), in a process called data-fusion. The FC can be a secondary base-station or even a CR. After the FC processes the data from the CRs, it decides upon the occupancy of the sensed channel. Centralized cooperative sensing can also be performed based on the hard decisions made by all cooperating CRs, in a process called decision-fusion. In this case, the binary decisions made by the CRs are combined at the FC using binary arithmetic before the final decision is arrived at. In both centralized schemes, the final decision is reported back to the CRs via a control channel, and an access algorithm takes place in the sequel. In distributed cooperative sensing, no FC exists and the decision is an iterative process performed by the cooperating CRs that communicate

among themselves. In the case of relay-assisted cooperative sensing, a given CR may serve as a relay to forward the sensing information from one CR to another, for centralized or distributed operation.

2.1. Spectrum sensing as a binary hypothesis test

The spectrum sensing can be formulated as a binary hypothesis test problem [7], i.e.

$$
\begin{aligned}
H_0 : \quad & \text{Primary signal is absent} \\
H_1 : \quad & \text{Primary signal is present,}
\end{aligned}
\tag{1}
$$

where H_0 is called the null hypothesis, meaning that there is no licensed user signal active in a specific spectrum band, and H_1 is the alternative hypothesis, which indicates that there is an active primary user signal [4].

Two important parameters associated with the assessment of the spectrum sensing performance are the probability of detection, P_{d}, and the probability of false alarm, P_{fa}, which are defined according to

$$
\begin{aligned}
P_{\mathrm{d}} &= \Pr\{\text{decision} = H_1 \mid H_1\} = \Pr\{T > \gamma \mid H_1\} \\
P_{\mathrm{fa}} &= \Pr\{\text{decision} = H_1 \mid H_0\} = \Pr\{T > \gamma \mid H_0\},
\end{aligned}
\tag{2}
$$

where $\Pr\{\cdot\}$ is the probability of a given event, T is the detection-dependent test statistic and γ is the decision threshold. The value of γ is chosen depending on the requirements for the spectrum sensing performance, which is typically evaluated through receiver operating characteristic (ROC) curves that show P_{fa} versus P_{d} as they vary with the decision threshold γ.

3. Detection techniques for spectrum sensing

In the context of spectrum sensing, the detection technique aims at extracting from the received signal a test statistic from which the spectrum occupancy is checked, as shown in (2). An overview of some of these techniques is given below:

- *Matched filter detection*: This technique maximizes the signal-to-noise ratio of the received signal and is considered the optimal one if the CR has prior knowledge about primary transmitted signal characteristics, such as the modulation order and type and the pulse shape [8]. If the channel is not a pure additive white Gaussian noise (AWGN) channel, the knowledge of the channel impulse response is needed as well. A matched filter has a challenging practical limitation which is related to the need of estimating or knowing *a priori* the abovementioned information. If such information is not sufficiently accurate, the spectrum sensing performs poorly.

- *Energy detection*: If prior information about the primary transmitted signal is unknown, the energy detection (ED) technique is the optimal one [9], [10]. After the received signal is filtered with a band-pass filter in order to select the desired bandwidth, it is squared and integrated over the sensing interval. The result, which is the test statistic, is compared with a decision threshold so that the absence or presence of the primary signal is inferred. Since this decision threshold depends on the thermal noise variance (noise power), even small noise variance estimation errors can lead to noticeable performance degradation.

- *Cyclostationary detection*: When the primary transmitted signal exhibits cyclostationarity, it can be detected by exploring the periodic behavior of the cyclostationary parameter. This method is more robust to noise uncertainty than energy detection [4],[11],[12]. Although a cyclostationary signal can be detected at lower signal-to-noise ratios compared to other detection strategies, cyclostationary detection is more complex than ED. Moreover, similar to the case of the matched filter detection, it requires some prior knowledge about the primary signal.

- *Eigenvalue-based detection*: Among the existing spectrum sensing detection techniques [6], eigenvalue-based schemes are receiving a lot of attention [13]-[15], mainly because they do not require prior information on the transmitted signal. In some eigenvalue-based schemes, the knowledge of noise variance is not needed either [15]. In eigenvalue spectrum sensing, the test statistic is computed from the eigenvalues of the received signal covariance matrix.

In this chapter we focus in the eigenvalue-based detection. The following techniques are addressed: the eigenvalue-based generalized likelihood ratio test (GLRT), the maximum-minimum eigenvalue detection (MMED), also known as the eigenvalue ratio detection (ERD), the maximum eigenvalue detection (MED), also known as Roy's largest root test (RLRT), and the energy detection (ED) [15]. Although ED is not an exclusively eigenvalue-based detection technique, it can be implemented using eigenvalue information.

Before presenting the specifics of the above eigenvalue-based detection techniques, a discussion about the spectrum sensing in the context of vehicular networks is in order. After this discussion the reader will hopefully be able to analyze the pros and cons of each detection strategy for applications in the vehicular network scenario.

4. Spectrum sensing in the scenario of vehicular networks

4.1. Vehicular Networks

The automotive industry is increasingly incorporating new functionalities to automobiles, aiming at improving the user's experience and safety. Some examples are the use of sensors to detect the proximity of another vehicle or object, automatic headlights and windshield wipers, speed alerts and speed limiters, cruise, traction and braking controls, etc. The majority of these functionalities, till now restricted to control mechanisms and to the interaction between the vehicle and the driver, are based on sensors, actuators and data processing tasks that make some decision or even provide some useful information.

Recently, there have been increased research efforts directed to the development of systems to support the interaction among different vehicles as well. One product of these efforts is the Intelligent Transportation System – ITS [16], which is intended to provide, among other things: traffic information, collision avoidance and congestion control in road transportation systems, as well as interfaces with other transportation systems.

Among the key elements of such intelligent transportation systems, communications play a vital role. A new class of wireless communications networks has emerged in this scenario: the vehicular *ad-hoc* network (VANET). It can be formed with vehicles, or with vehicles and a fixed communication infrastructure nearby the roads or streets. The applications of the VANETs can be focused mainly on *safety*, *entertainment* or *driver assistance* aspects:

- *Safety*: The promise for safety has been one of the main motivators for the development of vehicular networks. In general, the goal is to reduce the number and severity of the accidents by presenting related information to the driver or by actuating on some safety mechanism. Safety applications, however, pose some restrictions to the reliability and latency of the information presentation and actuations. Moreover, these applications must be robust against the presentation of false information and must be able to deal with conflicting data or decisions. Safety applications also must be able to deal with bad or unexpected situations, like the exchange of information about accidents on the road, poor visibility and slippery road, among others.

- *Entertainment*: Most of the applications oriented to entertainment in VANETs are associated to Internet access. This is because users are becoming more dependent on the Internet and they want to access it anywhere and anytime. Among the envisioned entertainment applications are short message services, music and video sharing, and multimedia distribution. In this sort of applications, latency is not a critical issue.

- *Driver assistance*: The main goal of this kind of application is to assist the driver by providing useful information, such as the availability of parking lots, locations in maps, alternative routes and touristic points.

Vehicular networks have some characteristics that distinguish them from other mobile wireless networks. Some of these characteristics are attractive to the network design; others represent important challenges. In the following items we present some of the attractive characteristics [17]; some challenges are listed in the sequel:

- *High transmit power*: Transmit power is not a strong restriction in VANETs, since the vehicle battery or outlets at the road's margins are capable of providing the necessary energy for the mobile and fixed parts of the network, respectively.

- *High computational power*: In principle, processing units with high computational power have no strong limitation of space and power supply in cars or in road units, which facilitates their implementation.

- *Mobility prediction*: Differently from other mobile networks, where it is practically impossible to predict the position of a device, in VANETs this prediction is simplified due to the fixed structure of roads and streets.

- The main challenges to the development of VANETs are [18]:

- *Large scale*: Differently from other *ad-hoc* networks, which normally assume a fixed and moderate size, VANETs can be extended to an entire road and can include a large number of participants.

- *High mobility*: The dynamic nature of the VANETs nodes is complicated when relative vehicle speeds can reach 300 km/h or even more, or when the vehicle density is largely increased, as happens during rush hours or traffic jams.

- *Fragmentation*: The dynamic nature of the VANETs nodes can also bring forth large gaps between vehicles, resulting in clusters of nodes isolated far apart from each other.

- *Topology and network connectivity problems*: Due to the fact that vehicles can constantly change their positions in a short time-frame, nodes are connected during short time intervals and connection loss increases. This represents a great challenge to the development of the network topology and connectivity management strategies.

- *Inadequate spectral bandwidth*: In spite of the fact that a large standardization effort is being put in the VANETs (e.g. in USA the Federal Communications Commission has allocated a 75 MHz band in the 5.9 GHz range for Dedicated Short Range Communications – DSRC [19]), specialists and researchers are claiming for bandwidths adequate to the increasing number and forms of the envisioned applications [20].

4.2. VANET architectures

The VANET architectures define the way in which nodes are organized and how they communicate. Before discussing about these architectures, it is convenient to establish the roles of two key elements of the network: the road site units (RSU) and the mobile nodes or vehicles [21]. The RSUs are part of the network infrastructure, and are typically located nearby roads and streets. They are responsible for providing communication within the VANET and between the VANET and other networks, like the Internet. These units can be public or belong to private service providers. Vehicles have a very important role in VANETs, as they are able to carry information to distant points in the network. Moreover, they are the main observers of the network surrounding environment, since accidents, traffic jams and other traffic events can occur out of reach of the fixed part of the network. In order for the vehicles to be able to monitor the road and traffic conditions, they must be equipped with some key components like sensors, processing and storage units, communication and positioning facilities and an appropriate user interface.

Basically, there are three main vehicular network architectures: pure *ad-hoc* (called vehicle-to-vehicle *ad-hoc* network – V2V), infrastructured[2] (also known as V2I) and hybrid. In V2V, vehicles communicate without any external support or centralizing element. In this architecture, vehicles act as routers or relays, forwarding data through multiple hops. The V2V

---

2 Althoug the VANET denomination suggests an exclusive association to ad-hoc networks, it has been used in the context of infrastrutured networks as well.

architecture is simpler, since it does not require infrastructure, but it is strongly influenced by vehicle density and mobility pattern, which can cause severe connectivity problems.

To avoid connectivity problems, the V2I architecture adopts static nodes distributed along the roads or streets. These nodes act as access points in IEEE 802.11 networks in structured mode, and centralize the network traffic, also serving as intermediate nodes for communication. The drawback of the V2I is the need of a large number of fixed elements installed along the road or street to improve connectivity, which increases system cost.

The hybrid architecture combines V2V and V2I. In the hybrid mode, a minimum fixed structure is used to increase connectivity e provide interconnection services. Besides the communication among vehicles and fixed parts, the hybrid architecture brings also the possibility of communication between vehicles via single or multiple hops.

4.3. Challenges and opportunities for spectrum sensing in the context of VANETs

One of the biggest challenges of large scale deployment of vehicular networks is the inadequate bandwidth assigned to it [20],[22]. Recent efforts have been put in the assignment of tens of megahertz in the 5.9 GHz band, which is the case of USA, Japan and Europe. However, specialists and researchers are claiming for more bandwidth for emerging services, like [22]:

- *Collision avoidance*: Signals with short durations (large bandwidths) are necessary for improving positioning and ranging, which are fundamental to avoid collisions.

- *Combating mobility*: High moving speeds can give rise to high Doppler spreads in the transmitted signal. This phenomenon can be alleviated with the use of high bandwidth signals, which will be proportionally less affected by a given Doppler spread than narrow-band signals.

- *Large volume of data*: Besides information on traffic, road condition, accidents and so on, data from Internet access can increase the demand for high data rates, also increasing the demand for higher bandwidths.

Recent studies have shown that around 70% of the spectrum assigned to TV broadcast in US is underutilized, mainly in small cities and in rural areas [23]. In roads nearby these places the underutilization can be even higher. A solution to the problem of spectrum underutilization and fixed spectrum allocation policy is to incorporate the cognitive radio concept into the context of vehicular networks. To this union it has been given the name Cog-VANET [22]. Similarly to other cognitive radio systems, Cog-VANETs face the challenge of having reliable and fast enough spectrum sensing capabilities. This challenge can be alleviated with the use of cooperative spectrum sensing, which is particularly promising in the Cog-VANET scenario due to the high diversity produced by the high mobility of vehicles [23],[24].

The benefits of the cooperative spectrum sensing to the Cog-VANETs were investigated in [20], [22] and [25]. In [20] the authors propose a CR-based architecture in which sensing information gathered by the vehicles is sent to fixed units at the road side (also called road units). The road units then send the sensing information to a central processing unit. In [25], it is suggested a new frame structure in which the spectrum sensing is considered in a coordinated fashion.

The coordination made by road units determines a group of channels to be sensed by each vehicle in the network. Since in both [20] and [25] it is assumed the presence of several fixed structures alongside the road, the cost can be prohibitive. On the other hand, in [22] the authors suggest a decentralized cooperative sensing in which each vehicle combines different sensing information from other vehicles in order to reach to a decision upon the occupancy of the sensed channel. However, due to the fact that the topology adopted is a V2V, there are inherent connectivity problems, as already mentioned in the previous subsection.

From above one can infer that a possible solution for the problem of spectrum sensing in cognitive vehicular networks would be a mix of centralized and decentralized (or distributed) techniques. Centralized ones would be preferred in regions with fixed structures nearby the roads or streets, whereas decentralized strategies would be preferred in regions without fixed units or with an inadequate density of them. Besides, the hybrid architecture would be the preferred one, since this would permit the communication between vehicles (V2V mode) and between vehicles and fixed units (V2I mode).

The high mobility of vehicles in Cog-VANETs, though advantageous from the perspective of the diversity gain when cooperative sensing is adopted, poses strong requirements in what concerns sensing time, computational power and spectrum agility. Sensing must be fast enough to be effective in this high mobility environment, which in one hand claims for simple detection techniques. On the other hand, the requirement for accuracy claims for more elaborated detection strategies, which in turn can require high computational power in order to keep the sensing time low. Last, radios must be agile in the sense that they must be able to switch between channels quickly. This imposes challenges to the transceiver design. A tradeoff among the above requirements seems to be the best solution, taking into account the centralized or distributed modes of operation that could be changing over time as a given vehicle moves through the network.

5. Centralized cooperative eigenvalue spectrum sensing

In this section we describe the centralized eigenvalue-based cooperative spectrum sensing models, considering the presence of impulsive noise. We first present the conventional model typically adopted in the literature, and then we discuss about a model oriented to the architecture of a real cognitive radio receiver. The impulsive noise models are also addressed in this section. The content of this section is partially based on [26].

Let's consider the well-known baseband memoryless linear discrete-time MIMO fading channel model. Assume that there are m antennas in a CR, or m single-antenna CRs, each one collecting n samples of the received signal from p primary transmitters during the sensing period. Consider that these samples are arranged in a matrix $\mathbf{Y} \in X^{m \times n}$. Similarly, consider that the transmitted signal samples from the p primary transmitters are arranged in a matrix $\mathbf{X} \in X^{p \times n}$. Let $\mathbf{H} \in X^{m \times p}$ be the channel matrix with elements $\{h_{ij}\}$, $i = 1, 2, \ldots, m$ and $j = 1, 2, \ldots, p$, representing the channel gain between the j-th primary transmitter and the i-th sensor (antenna

or receiver). Finally, let $\mathbf{V}$ and $\mathbf{V}_{\mathrm{IN}} \in X^{m \times n}$ the matrices containing thermal noise and IN samples that corrupt the received signal, respectively. The matrix of received samples is then

$$\mathbf{Y} = \mathbf{HX} + \mathbf{V} + \mathbf{V}_{\mathrm{IN}}. \qquad (3)$$

In eigenvalue-based sensing, spectral holes are detected using test statistics computed from the eigenvalues of the sample covariance matrix of the received signal matrix $\mathbf{Y}$. If a multi-antenna device is used to decide upon the occupation of a given channel in a non-cooperative fashion, or even in a centralized cooperative scheme with data-fusion, matrix $\mathbf{Y}$ is formed, and the sample covariance matrix

$$\mathbf{R} = \frac{1}{n} \mathbf{Y}\mathbf{Y}^{\dagger} \qquad (4)$$

is estimated, where † means complex conjugate and transpose. The eigenvalues $\{\lambda_1 \ge \lambda_2 \ge \ldots \ge \lambda_m\}$ of $\mathbf{R}$ are then computed, and assuming a single primary transmitter ($p = 1$), the test statistics for GLRT, MMED, MED, and ED are respectively calculated according to [15]

$$T_{\mathrm{GLRT}} = \frac{\lambda_1}{\frac{1}{m}\mathrm{tr}(\mathbf{R})} = \frac{\lambda_1}{\frac{1}{m}\sum_{i=1}^{m}\lambda_i}, \qquad (5)$$

$$T_{\mathrm{MMED}} = \frac{\lambda_1}{\lambda_m}, \qquad (6)$$

$$T_{\mathrm{MED}} = \frac{\lambda_1}{\sigma^2}, \qquad (7)$$

$$T_{\mathrm{ED}} = \frac{\|\mathbf{Y}\|_F^2}{mn\sigma^2} = \frac{1}{m\sigma^2}\sum_{i=1}^{m}\lambda_i, \qquad (8)$$

where σ^2 is the thermal noise power, assumed to be known and with equal value in each sensor input, and tr( ) and $\|\ \|_F$ are the trace and the Frobenius norm of the underlying matrix, respectively.

All the eigenvalue-based detection methods rely on the fact that, asymptotically in n, the sample covariance matrix $\mathbf{R}$ in the presence of noise only is a diagonal matrix with all its non-zero elements equal to σ^2. Hence, $\mathbf{R}$ has eigenvalues equal to σ^2 and multiplicity m [27]. In the

presence of a primary user, this is no longer true, and these detection methods try to identify this situation: as one can see in (5), in GLRT the ratio between the largest eigenvalue and the average of all the remaining ones is computed; in MMED the ratio between the largest and the smallest eigenvalues is computed; in MED it is assumed that the noise variance σ^2 is known, and the largest eigenvalue is compared with σ^2.

5.1. Conventional model

In the conventional discrete-time memoryless MIMO model (*C-model*), when a centralized cooperative sensing with single-antenna cognitive radios is considered, the matrix with received signal samples **Y** in (3) is presumed to be available at the fusion center as if no signal processing is needed before each row of **Y** is forwarded to the FC by each CR. A simulation setup under *C-model* just considers that **Y** is available to the FC as is.

5.2. Implementation-oriented model

A more realistic model was originally proposed in [28] and called *implementation-oriented model*. It considers typical signal processing tasks performed by each CR before the collected sample values are sent to the FC. The diagram shown in Figure 3 was the main reference for constructing such a model. A wideband band-pass filter (BPF) selects the overall spectrum range to be monitored. The low noise amplifier (LNA) pre-amplifies small signals and a down-conversion (DC) process translates the received signal to in-phase and quadrature (I&Q) baseband signals. The local oscillator (LO) is part of the down-conversion circuitry. A variable-gain amplifier (VGA), which is part of an automatic gain control (AGC) mechanism, is responsible for maintaining the signal within the dynamic range of the analog-to-digital converter (ADC). The channel low-pass filter (LPF) selects the desired spectrum fraction to be sensed. Since filtering affects signal correlation, a whitening process takes place to guarantee that noise samples are decorrelated when the test statistic is computed. This is necessary because the test statistics considered herein implicitly assume decorrelated noise samples.
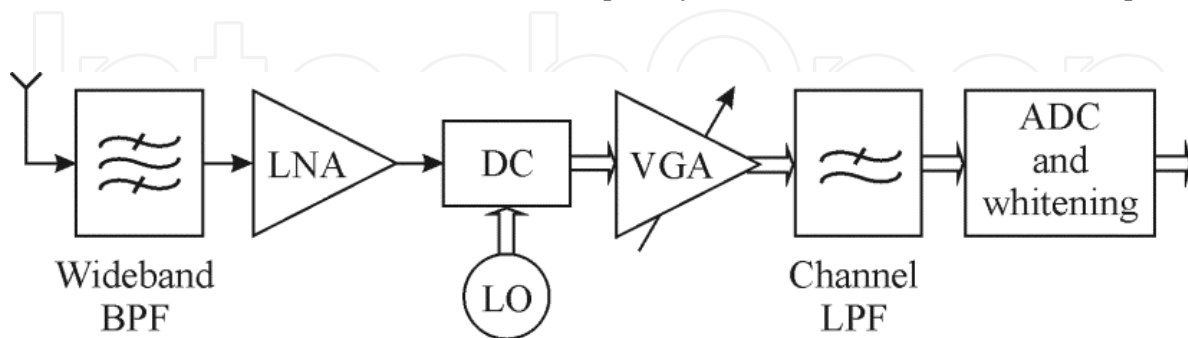

Figure 3. CR receiver diagram (adapted from [28]).

The simulation setup under the realistic implementation-oriented model (*R-model*) has been built to mimic the system diagram shown in Figure 3, in which the down-conversion (DC) to baseband is assumed ideal, as also implicitly assumed in the conventional model. A

non-ideal down-conversion in which a direct-conversion receiver (DCR) model is adopt-ed is considered in [28].

Matrices $\mathbf{X}$, $\mathbf{H}$, $\mathbf{V}$, and $\mathbf{V_{IN}}$ under the *R-model* are generated as described in the following subsections.

5.2.1. Transmitted signal

To simulate a Gaussian-distributed noise-like transmitted signal with controllable time correlation, matrix $\mathbf{X}$ in (3) is formed by filtering independent and identically distributed (i.i.d.) complex Gaussian samples with a length-L moving average (MA) filter with no quantization (using floating-point computation). This type of filter was chosen for reasons of simplicity; any other low-pass filter could be adopted as well. The memory elements in the structure of this and subsequent MA filtering processes are assumed to have zero initial value before the first valid sample is applied to their inputs. As a result, the first $(L-1)$ samples resulting from the MA filtering, out of $(n+L-1)$, are discarded before subsequent operations. The Gaussian distribution for the entries of $\mathbf{X}$ was adopted because it accurately models several modulated signals, for instance the amplitude of a multicarrier signal, such as orthogonal frequency-division multiplexing (OFDM), with a large number of subcarriers, which is the preferred modulation technique in most modern wireless technologies, including several digital television standards. The time correlation introduced by the MA filter models the limited bandwidths of the transmitted and received signals, which are proportional to the symbol rate.

5.2.2. Channel

The elements in the channel matrix $\mathbf{H}$ in (3) are zero mean i.i.d. complex Gaussian variables that simulate a flat Rayleigh fading channel between each primary transmitter and sensor (cognitive radio), assumed to be constant during a sensing period and independent from one period to another.

5.2.3. Receive filters

To take into account the effect of the CR receive filters on the thermal and impulsive noises, the entries in $\mathbf{V}$ and $\mathbf{V_{IN}}$ in (3) are MA-filtered complex Gaussian variables that represent, respectively, the colored additive thermal noise and the impulsive noise at the output of the receive filters.

A normalization of filtered samples was done to guarantee the desired received signal-to-noise ratio (SNR), in dB, and the desired average IN power. Specifically, $\mathbf{X} \leftarrow \mathbf{X}/P_X^{1/2}$ for unitary average received signal power, $\mathbf{V} \leftarrow \mathbf{V} \times P_V^{-1/2} \times 10^{-SNR/20}$ for an SNR-dependent average thermal noise power, and $\mathbf{V_{IN}} \leftarrow \mathbf{V_{IN}} \times P_{VIN}^{-1/2} \times K^{1/2} \times 10^{-SNR/20}$ for an average IN power K times the thermal noise power, where $\leftarrow$ represents the normalization process, P_X, P_V, and P_{VIN} are the average time-series powers in $\mathbf{X}$, $\mathbf{V}$, and $\mathbf{V_{IN}}$ before normalization, respectively. Moreover, to guarantee the desired received SNR, matrix $\mathbf{H}$ is normalized so that $(1/mp)||\mathbf{H}||_F^2 = (1/mp)\text{tr}(\mathbf{H}^\dagger\mathbf{H}) = 1$.

5.2.4. LNA and AGC

The effect of the LNA and the AGC on the samples processed by the i-th CR, $i = 1, 2, …, m$, is given by the gain

$$g_i = \frac{f_{od}D\sqrt{2}}{6\sqrt{\frac{1}{n}\mathbf{y}_i^\dagger \mathbf{y}_i}} = \frac{f_{od}D\sqrt{2n}}{6\|\mathbf{y}_i\|_2}, \tag{9}$$

where $\mathbf{y}_i$ is the i-th row of $\mathbf{Y}$, i.e., the set of n samples collected by the i-th CR, and $\|\mathbf{y}_i\|_2$ is the Euclidian norm of $\mathbf{y}_i$. The reasoning behind the definition of these gains is explained as follows: The combined gains of the LNA and the AGC are those that maintain the signal amplitude at the inputs of the in-phase and quadrature ADCs within their dynamic ranges D. By dividing the sample values by the square root of $\mathbf{y}_i^\dagger \mathbf{y}_i/n$, which is the average power of $\mathbf{y}_i$, one obtains a sequence with unitary average power. Since $\mathbf{X}$ have complex Gaussian entries, $\{\mathbf{y}_i\}$ have complex Gaussian distributed sample values, conditioned on the corresponding channel gain. If σ^2 is the variance of these samples after the effect of the LNA and the AGC, to guarantee that six standard deviations (practically the whole signal excursion or 99.73% of the sample values) of the I&Q signals will be within $[-D/2, D/2]$, we shall have $6(\sigma^2/2)^{1/2} = D$, which means that the signal power at the output of the AGC will be $\sigma^2 = 2D^2/36$. This justifies the factor $(2^{1/2}D)/6$ in (9). Finally, as the name indicates, the overdrive factor $f_{od} \geq 1$ is included as a multiplier in (9) to simulate different levels of signal clipping caused by real ADCs, i.e., it produces signal amplitudes greater than or equal to 6σ. For example, an $f_{od} = 1.2$ means that the dynamic ranges of the signals at the input of the ADCs will be 20% larger than the dynamic ranges of the ADC's inputs. The I&Q clippings act on each sample value s applied to their inputs according to $s \leftarrow \text{sign}(s)\times\min(|s|, D/2)$.

5.2.5. Whitening filter

The Whitening filter matrix $\mathbf{W}$ [29] that multiplies the MA-filtered, amplified and perhaps clipped versions of $\{\mathbf{y}_i\}$ is computed with floating point according to $\mathbf{W} = \mathbf{U}\mathbf{C}^{-1}$, where $\mathbf{U}$ is the orthogonal matrix from $\mathbf{Q} = \mathbf{U}\mathbf{\Sigma}\mathbf{K}^T$, the singular-value decomposition of the receive filter covariance matrix $\mathbf{Q}$. The elements of $\mathbf{Q}$ are $Q_{ij} = a_{|i-j|}$, with a_k representing the discrete autocorrelation function of the MA filter impulse response, i.e. $a_k = (1 - k/L)$, for $k \leq L$, and $a_k = 0$ otherwise, for $i, j, k = 0, 1, …, (n-1)$. Matrix $\mathbf{C}$ is the lower triangular matrix from the Cholesky decomposition of $\mathbf{Q}$.

5.2.6. ADC, transmission to the FC and decision

The effect of the analog-to-digital conversion on the processed sample values that will be sent to the FC is modeled by a quantizer with configurable number N_q of quantization levels. One must be aware that in practice there will be two ADC operations: the above-described one and the ADC operation with the aim of digital signal processing tasks locally at each CR.

Assuming no bit errors in the reporting channels, the modified received matrix $\mathbf{Y} = \mathbf{HX} + \mathbf{V} + \mathbf{V}_{IN}$ in the implementation-oriented model is then formed at the FC, from which the sample covariance matrix $\mathbf{R}$ is computed, and then the eigenvalues $\{\lambda_i\}, i = 1, \ldots, m$. The test statistics for GLRT, MMED, MED, and ED are respectively computed from (5), (6), (7), and (8). In each detection technique, the corresponding test statistic is compared with a threshold computed from the desired false alarm probability, and a final decision upon the occupancy of the sensed channel is reached.

5.3. Impulsive noise model

Impulsive noise can be i) generated from the electrical mains or by direct induction on the receiver, or ii) captured by the receiver antenna. In the first category, the main noise sources are the ignition system of ovens, the control system of dishwasher machines, thermostats of heaters, and switches of fluorescent and incandescent lamps. In the second category, typical sources are lightning and the ignition system of cars, which is particularly relevant in the vehicular network scenario.

Several models are available in the literature for characterizing IN [30]-[34]. Firstly, we discuss about the one presented in [31], in which the IN waveform is generated by properly gating a white noise signal, as illustrated in Figure 4. The main parameters that govern the IN waveform are also shown in this figure. They are configured according to the noise source type, as described in detail in [31].
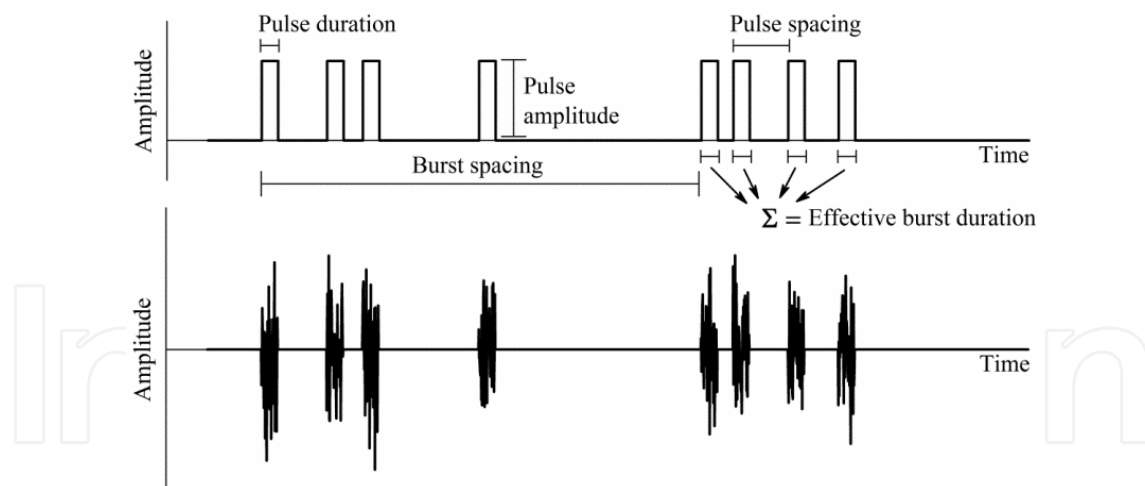

Figure 4. Gating waveform (top) and impulsive noise waveform (bottom) (From [26]).

To adhere the above parameters to the context of spectrum sensing, we have translated them into five other parameters: K is the ratio between the time-series average IN power and the average thermal noise power; p_{IN} denotes the probability of occurrence of IN during a given sensing period, and p_{CR} represents the fraction of CRs hit by IN. As a result, the probability of the occurrence of IN is a Bernoulli random variable with probability of success p_{IN}, and the number of CRs independently hit by IN is a binomial random variable with parameters m and

p_{CR}. A configurable number N_b of IN bursts occurs during a sensing period, each burst having configurable length N_s, i.e., each IN burst corrupts N_s consecutive samples collected by a given CR. The separation between consecutive bursts is uniformly distributed in the discrete-time interval [0, $n - N_b \times N_s$].

An alternative impulsive noise model was proposed in [33] and [34]. The parameters K, p_{IN} and p_{CR} previously defined are also used in this model, so that it fits to the scenario of cooperative spectrum sensing. The first assumption is the use of an exponential distribution with parameter β in order to settle the interval between impulsive noise pulses. Thus, to compute the number of samples separating each pulse, a random number distributed according to an exponential density with parameter β samples is generated. The pulse amplitudes follow a lognormal distribution. With the purpose of generating the IN amplitude values, a Gaussian random variable Z with mean equal to A dBμV and standard deviation B dB is generated. Then, the value $Z = z$ dBμV is converted to its equivalent amplitude z μV, which is a log-normal variable, using the transformation $z[\mu V] = 10^{z[dB\mu V]/20}$. The phase of the impulsive noise is modeled using a uniformly-distributed random variable θ in (0, 2π]. Since z is the amplitude, the in-phase and quadrature components of the IN are respectively given by $I_I = z\cos\theta$ and $I_Q = z\sin\theta$.

Figure 5 depicts an example of the compound (thermal plus impulsive) noise waveform (real part) generated according to the model proposed in [33] and [34]. In this figure, the mean of the pulse magnitude A = 70 dBμV, the standard deviation of the pulse magnitude B = 8.5 dB, β = 900 samples (which means that it is expected one impulsive noise pulse every 900 samples, on average), Gaussian thermal noise root mean square power 50 dBμV and total generation time of 2 seconds.
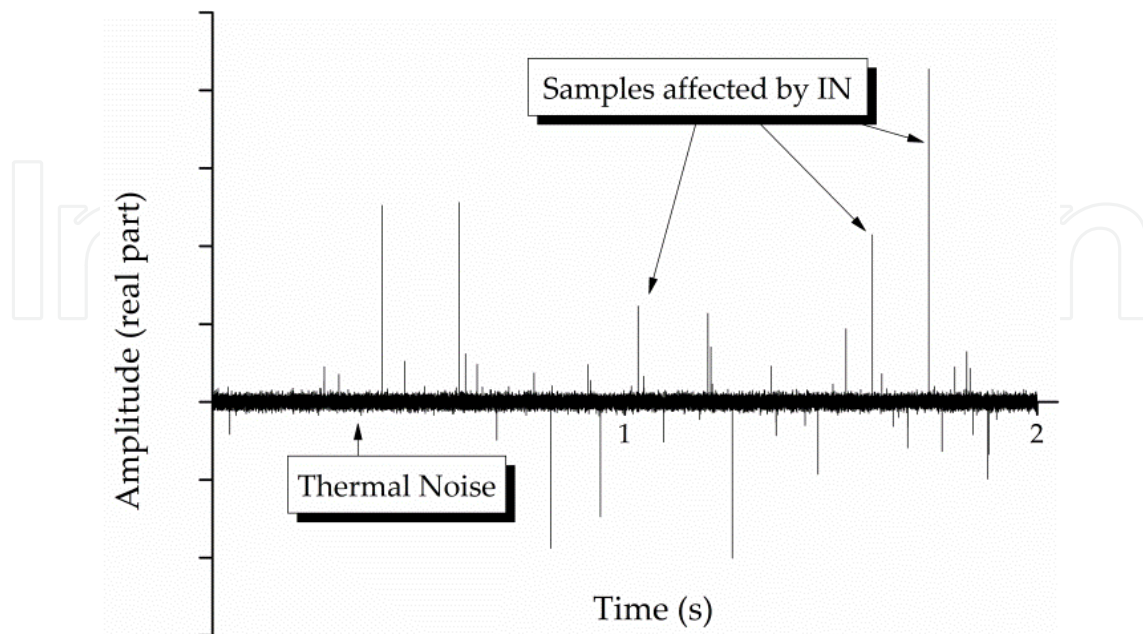

Figure 5. Illustration of the compound (thermal plus impulsive) noise waveform generated by the simulation platform.

6. Description of the simulation platform

This section describes the MATLAB-based simulation platform[3] that provides interactive access to the performance analysis of the four spectrum sensing techniques considered in this chapter: MED, MMED, GLRT and ED. The platform GUI (graphical user interface) is showed in Figure 6.

Figure 6. The MATLAB-based simulation platform GUI.

In order to be prompted with the GUI, one must run the file "Main_Spectrum_Sensing.m" in the MATLAB environment. As detailed in the previous sections, there are a large number of scenarios and, consequently, a large number parameters to be set.

First it is necessary to configure the box *System Configuration*, where the model (conventional, *C-model* or the realistic implementation-oriented, *R-model*) can be chosen. In both cases the simulation can be performed with or without impulsive noise.

In the case of the *C-model*, the parameters to be configured are:

• the numbers of CRs (m),

• the number of samples collected from the received signal in each CR (n),

- the number of Monte Carlo simulation events (N_e); the choice of a large N_e will improve the accuracy of the results but will increase the simulation runtime,

- the sensing technique under analysis (MED, MMED, GLRT, ED or user customized sensing technique), and

- the type of transmitted signal (noise, BPSK, QAM or user defined modulation).

If the *R-model* is selected, additional parameters to be configured are:

- the number of quantization levels (N_q),

- the ADC dynamic range (D),

- the overdrive factor (f_{od}), and

- the filter length (L).

If the user intends to simulate the IN influence, the following IN parameters have to be set:

- probability of IN occurrence (p_{IN}),

- fraction of CRs hit by IN (p_{CR}),

- number of samples affected by IN (N_s),

- number of IN bursts (N_b), and

- the ratio between the average IN power and the average thermal noise power (K).

If the user aims to simulate the alternative IN model effect, only the parameter K, p_{IN} and p_{CR} will be used from the previous IN model. Additionally the user has to set:

- the average number of samples between impulsive noise pulses (β),

- the mean of the log-normal impulsive noise amplitudes (A), and

- the standard deviation of the log-normal amplitudes (B).

In the first simulation possibility, called here *Simulation 1*, the user has to configure a fixed SNR value in dB and the decision threshold range (minimum and maximum values). It is also possible to set the number of threshold values (default 8) within the threshold range. This will be the number of points in the graphs prompted at the end of a simulation.

To run the simulation, one must click the *Process* button. There is a countdown timer that appears in the "System Message" in the MATLAB GUI when the simulation is in progress. This counter is used to check the status of the simulation. If it is necessary to stop the processing, just press "*Ctrl + C*".

After processing, the simulation platform can return three graphs: P_d and P_{fa} as a function of the threshold range, the receiver operating characteristic (ROC) curve, P_d versus P_{fa} and histograms of the test statistic under the hypothesis H_0 and H_1.

In the second simulation option, named *Simulation 2*, three parameters s have to be defined: a fixed threshold, the minimum and the maximum SNR values and the number of points within

the SNR range (default 8). After processing, one graph is prompted, which shows P_d and P_{fa} as a function of the SNR range.

It is possible to save all the generated data by the simulation as a ".dat" file. This file contains three columns: P_d, P_{fa} and the threshold range if the *Simulation 1* is performed; and P_d, P_{fa} and the SNR range if the *Simulation 2* is performed. Additionally, a file with all the system parameter used in the simulations is saved as a ".dat" file. A dialog box enables the user to provide a prefix for the name of both files; they are saved as "*prefix_results.dat*" and "*prefix_parameters.dat*".

The platform can be easily customized so that the user can choose situations and settings different from the default ones. As an example, are possible to define any type of transmitted signal covariance matrix. Currently, there are three types of such signals: noise, BPSK and MQAM. However, in the *transmitted signal* drop-down list there is a fourth option that can be selected. When this occurs, a other window is prompted to let the user select a ".dat" file, which must contain the desired complex transmit symbols. For example, assume that it is necessary to simulate an MPSK transmitted signal. To do this, simply load a custom ".dat" file with a vector containing the *M* complex MPSK symbols. In such a way, the user will have flexibility to choose any type of transmitted signal, expanding the capabilities of the simulation platform. Other customization features like this will be included in new versions of the platform, and will be made available at http://www.inatel.br/lambdaproject.

As another example of customization, suppose that it is desired to include a new detection technique besides MMED, MED, GLRT and ED. From the menu *Sensing Technique*, select the option *Customized*. The user will be guided to the module (function) for the generation of the test statistic, called "*Gen_Var_T.m*", as illustrated in Figure 7. In the box identified as *Customized User Technique* the user must insert the formula for the computation of the new test statistic *T*, having as inputs any of the variables *m*, *n*, **Y**, $\{g_i\}$, SNR and $\{\lambda_i\}$ defined in Section 5 and commented in the body of the simulation source code.

```
%%%%% GLRT %%%%%
case 5
    T = lambda(1) / (sum(diag(W))/m);
%%%%% Customized User Technique %%%%%
case 6
    %T = ?;
otherwise
    null; end
```

Figure 7. Part of the simulation source code highlighting the generation of the test statistic *T*.

Different customization features can also be included due to the modular structure of the program exemplified in Figure 7. For example, the sensing performance can be evaluated considering correlated shadowing, fast fading, composite fading, different statistical models of the channel, different types of filters, etc. To perform such additional customization the user must modify the corresponding module of the program. For example, suppose that the user want to assess the spectrum sensing performance in a channel other than the already available

flat Rayleigh fading channel. To do that, the user must modify the module "*Gen_Channel_H.m*". Figure 8 shows the source code for the channel model before (left) and after (right) a customization. For the sake of simplicity and didactical purposes, the new channel model has been chosen as a fixed flat channel with unitary gain. A large number of channel models are available in the literature, but particularly in the case of vehicular networks, the user should refer to [35]-[37] and references therein.

```
function [H] = Gen_Channel_H(m,p)          function [H] = Gen_Channel_H(m,p)
%Returns Channel array H(mxp) with         %Returns Channel array H(mxp) with
%Rayleigh Normalized samples. Input : m    %Rayleigh Normalized samples. Input : m
%(number of CR ; p(number of primary       %(number of CR ; p(number of primary
%user) Output: array H (mxn)               %user). Output: array H (mxn)
%Generates normalized Rayleigh Channel     %Generates normalized Rayleigh Channel
H = sqrt(2)/2* randn(m,p) +  j *           %H = sqrt(2)/2* randn(m,p) +  j *
sqrt(2)/2* randn(m,p);                     %sqrt(2)/2* randn(m,p);
PH =                                       %PH =
1/(m*p)*sum(diag(ctranspose(H)*H));        1/(m*p)*sum(diag(ctranspose(H)*H));
H = H / sqrt(PH);                          %H = H / sqrt(PH);
                                           %%New channel entered by user
                                           H = ones(m,p)
```

Figure 8. Source code of the module responsible for synthesizing the channel model: before customization (left), after a didactical customization (right).

7. Some numeric results about the influence of the system parameters

In this section we present simulation results and a brief discussion concerning the influence of the system parameters under the *C-model* and *R-model* on the spectrum sensing performance for GLRT, MMED, MED, and ED. All the graphs were obtained from the simulation platform described in Section 6.

It is worth mentioning that the ROC curves for all the detection techniques under the *C-model*, for $m = 6$, $n = 50$, and SNR = –10 dB, are in agreement with those reported in [15].

The ROC curves shown hereafter were obtained with a minimum of 15,000 runs in Monte Carlo simulations implemented according to the setup described in Section 5.

Figure 9 shows empirical probability density functions (histograms) of the test statistic generated from the simulation platform using the energy detection and *C-model*, for $m = 6$, $n = 50$, and $p = 1$, and for SNR = –10 dB (left) and SNR = 0 dB (right). The histograms depict the hypotheses H_0 (primary signal absent) and H_1 (primary signal present). One can notice that P_d increases with an increased SNR, considering a fixed threshold, since the area of the histogram on the right of a given threshold under H_1 increases. The net result is an improved (increased) P_d for a given P_{fa} or an improved (reduced) P_{fa} for a given P_d.

Figure 10 shows ROC curves under *C-model* for different values of the number of collected samples (n), relating the probability of false alarm (P_{fa}) and the probability of detection (P_d) for
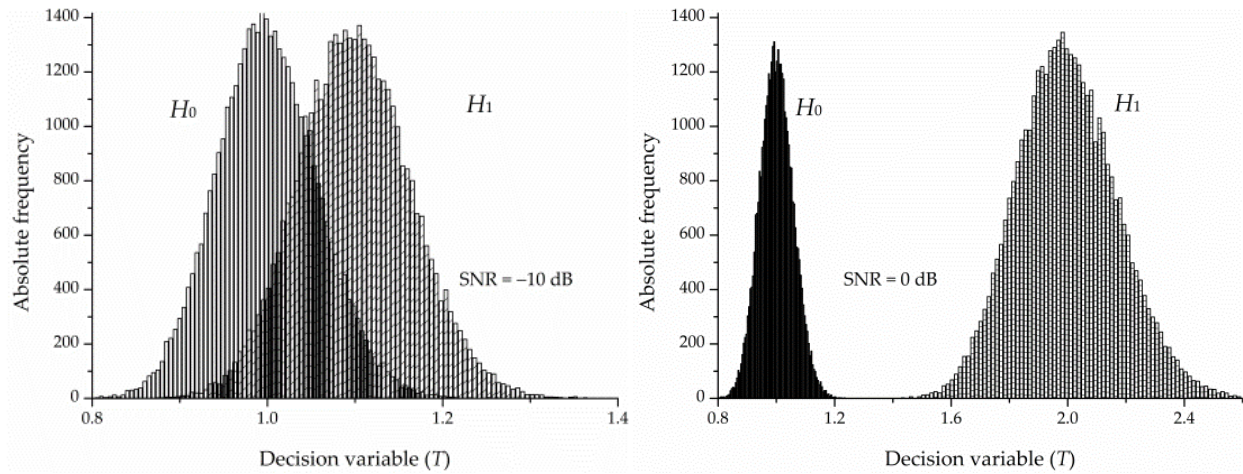
Figure 9. Histograms of the test statistic for ED under different SNR values.

MMED. Clearly, the influence of increasing the number n of collected samples per CR is a performance improvement, considering as fixed the remaining parameters. The threshold range for γ were 2.8 to 4.35 for $n = 60$, 2.8 to 5.1 for $n = 50$, and 2 to 6.5 for $n = 40$. One can notice that the greater the maximum threshold, the smaller P_d and P_{fa}. In the same way, for smaller minimum threshold, P_d and P_{fa} tend to 1. All the fixed remaining parameters are identified in the graph.
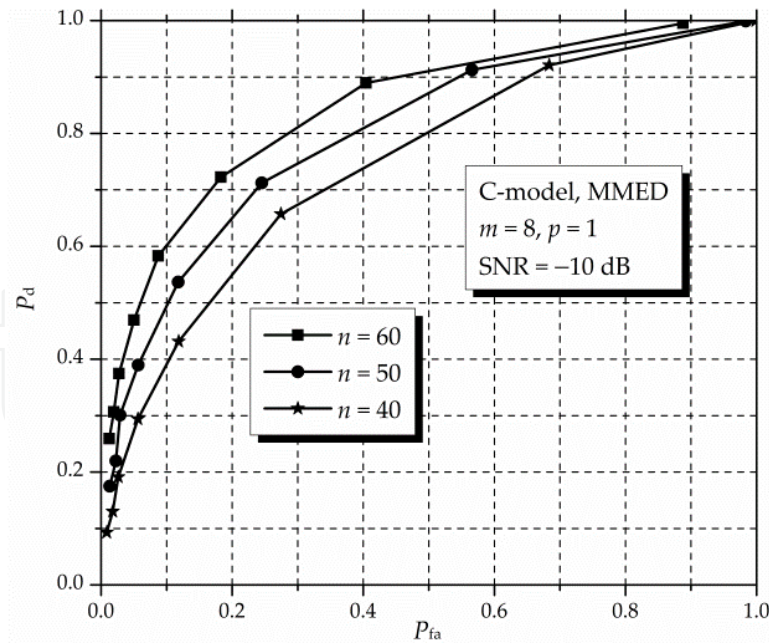

Figure 10. ROC curves for MMED (or ERD) and variable number of collected samples (n) under *C-model*.

In Figure 11 it is plotted two curves under *C-model* for a fixed value of the number of collected samples ($n = 50$), relating the false alarm probability (P_{fa}) and the detection probability (P_d) as

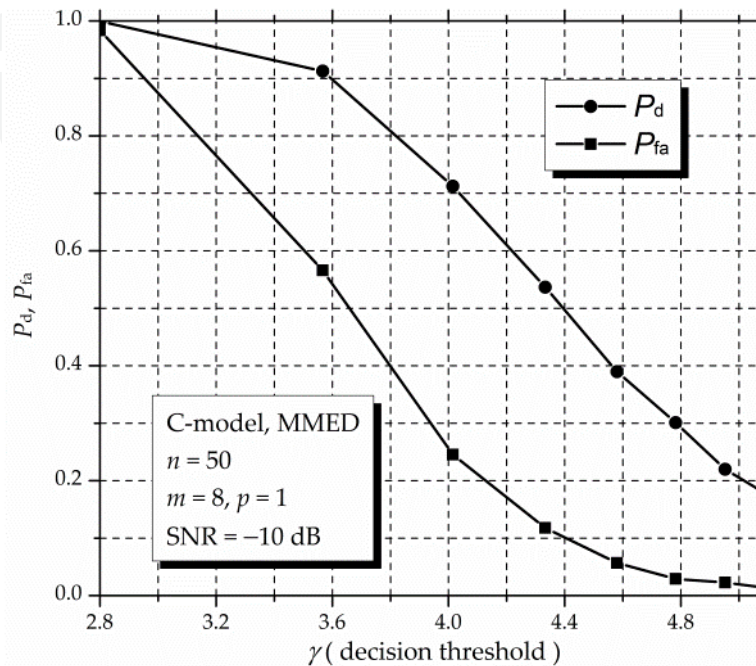a function of the decision threshold γ for MMED. All the remaining parameters are identified in the graph.

Figure 11. P_d and P_{fa} versus decision threshold γ for MMED (or ERD) for variable number of collected samples (n) under *C-model*.

Now, in order to check the influence of the SNR, Figure 12 depicts some curves under *C-model* for different values of the number of CRs (m), relating the detection probability (P_d) and the signal-to-noise ratio SNR for the RLRT. As expected, the influence of increasing the number of CRs is a performance improvement for a given SNR, considering as fixed the remaining system parameters. On the other hand, one can notice from Figure 12 that for a fixed m, the detection probability increases with the increase of the SNR. All the fixed remaining parameters are identified in the graph.

8. Some numeric results about the influence of the impulsive noise

In this section, further results obtained from the simulation platform are presented and discussed, now for a scenario with IN. We have used only the IN model proposed in [31], since practically the same results were obtained with the alternative model proposed in [33] and [34].
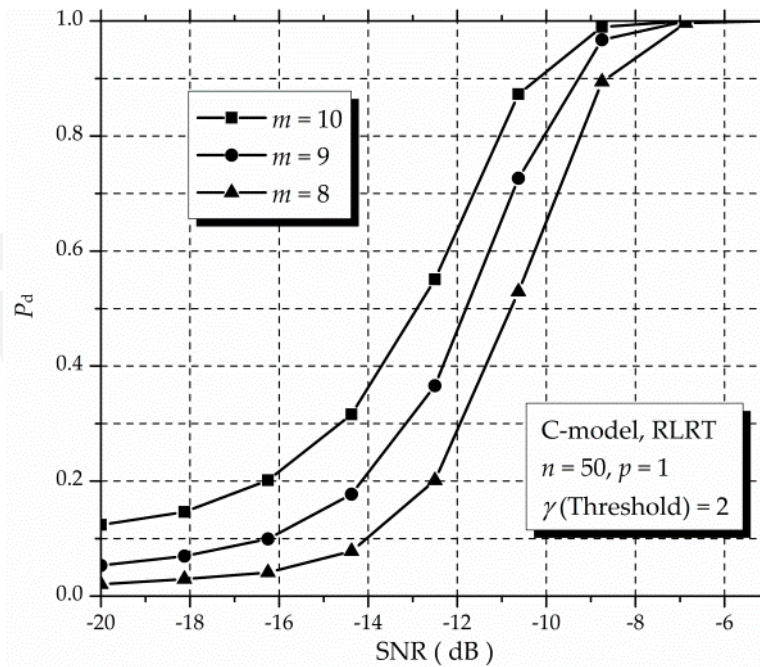
Figure 12. P_d versus SNR for RLRT for variable number of CRs (m) under *C-model*.

As can be seen in Figure 13, under the *C-model* and considering GLRT, impulsive noise degrades the performance for all false alarm probability values. That is, for a fixed P_{fa} the detection probability decreases with an increased impulsive noise power factor K (the ratio between the time-series average IN power and the average thermal noise power). The ranges of decision thresholds used for plotting these ROC curves were 1 to 1.9 for $K = 0$ and $K = 0.5$, and 1 to 2.05 for $K = 1$. All the fixed remaining system parameters are identified in the graph.

In Figure 14, which considers the *C-model* and the GLRT, one can notice that impulsive noise progressively degrades the performance for all false alarm probability values with an increase in the probability of impulsive noise occurrence. The ranges of decision thresholds used for plotting these ROC curves were 1.3 to 1.81 for $p_{IN} = 0.2$, 1.3 to 1.845 for $p_{IN} = 0.4$, 1.3 to 1.98 for $p_{IN} = 0.6$, and 1.3 to 2 for $p_{IN} = 0.8$. All the remaining fixed parameters are identified in the figure.

Now, in order to show a numerical result with *R-model*, Figure 15 presents some ROC curves considering different values for the number of quantization levels N_q, under IN. The range of decision thresholds used for plotting Figure 15 was 1.28 to 1.82 for all quantization levels N_q. It can be seen that the performance of the sensing scheme is worse for $N_q = 4$, changing slightly from $N_q = 8$ up to $N_q = 32$.

Finally, it is worth mentioning that different values of the system parameters and scenarios can lead to different performances. Thus, a myriad of different scenarios can be exercised through the proposed simulation platform. In this chapter we have just analyzed some parameter variations and scenarios, with the unique objective of showing the applicability of the platform. For a more complete analysis, the reader should refer to [26] and [28].
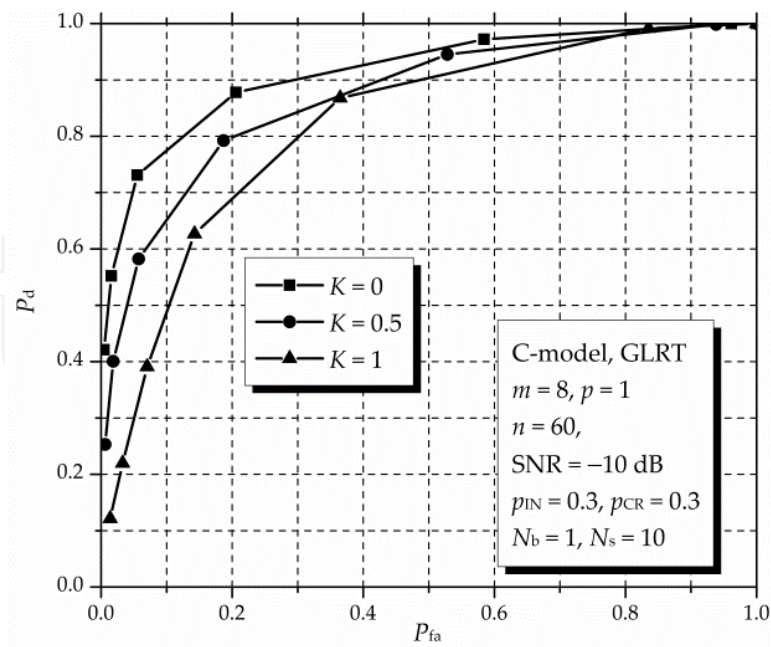
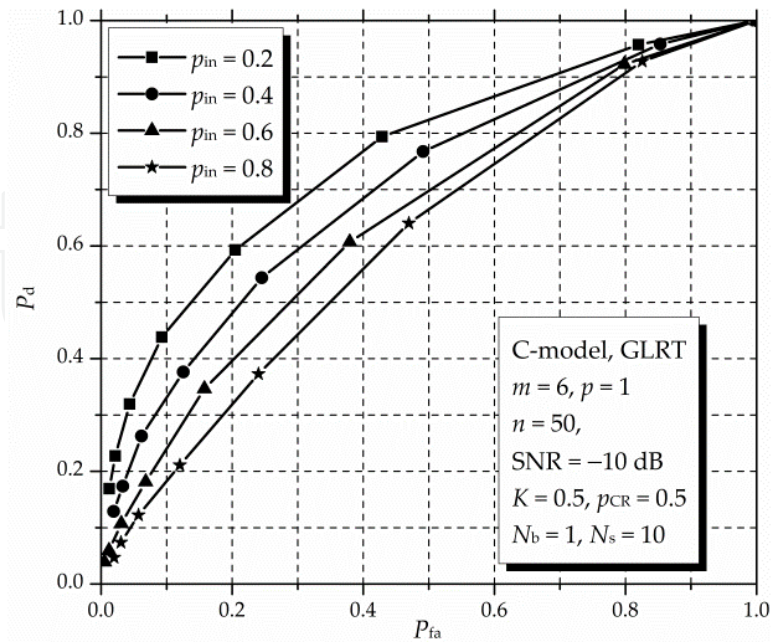**Figure 13.** ROC curves for GLRT with and without IN under *C-model*.

Figure 14. ROC curves for GLRT with IN under p_{IN} variations for C-model.

The figure shows ROC curves with P_d on the vertical axis (0.0 to 1.0) and P_{fa} on the horizontal axis (0.0 to 1.0). Legend: $N_q = 32$, $N_q = 16$, $N_q = 8$, $N_q = 4$. Annotation box:

C-model, GLRT
$m = 6$, $p = 1$
$n = 50$, SNR $= -10$ dB
$K = 0.3$,
$p_{CR} = 0.5$, $p_{IN} = 0.2$
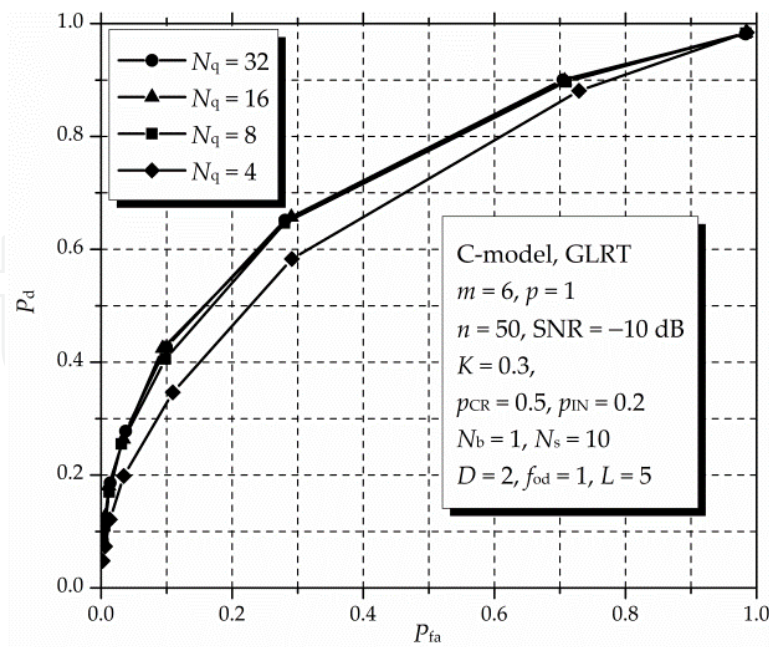$N_b = 1$, $N_s = 10$
$D = 2$, $f_{od} = 1$, $L = 5$

Figure 15. ROC curves for GLRT with IN under N_q variations for *R-model*.

9. Concluding remarks

This chapter described a MATLAB-based simulation platform for assessing the performance of cooperative spectrum sensing in cognitive radio applications such as in vehicular technology applications (e.g. V2V and V2I). The platform is flexible, allowing for the simulation of several sensing techniques, under a broad combination of system parameters. The focus was the cooperative techniques based on the eigenvalues of the received signal, such as GLRT, MMED, and MED, but the customizable feature of the simulation platform allows for the implementation and assessment of new detection techniques. The simulation can be configured to consider a conventional model in which no signal processing is performed by each cooperating CR, or to consider a more realistic approach in which typical CR signal processing tasks are taken into account. It can also simulate a scenario with impulsive noise corrupting the received samples in each CR. Besides the possibility of customizations already implemented in the platform, the modular structure of the program permits new ones to be easily included.

Besides the description of a simulation platform, this chapter reviewed basic concepts related to the spectrum sensing process for cognitive radio applications, and discussed the use of spectrum sensing in the context of cognitive vehicular networks. From this discussion it was possible to infer that the high mobility of vehicles in these networks, though advantageous from the perspective of the diversity gain when cooperative sensing is adopted, poses strong requirements in what concerns sensing time, computational power and spectrum agility. Sensing must be fast enough to be effective in this high mobility environment, which in one hand claims for simple techniques like the energy detection. However, the sensitivity of the

energy detection to noise variance uncertainty can drastically degrade its performance. On the other hand, the requirement for accuracy claims for more elaborated detection strategies that do not need noise variance estimation, as is the case of some eigenvalue-based ones, which in turn can require high computational power to keep the sensing time low. The balance between low complexity and accuracy of the spectrum sensing process is shown to be a formidable research challenge in the scenario of vehicular networks, opening the possibility of new ideas or the improvement of old ones.

Author details

Rausley Adriano Amaral de Souza[*], Dayan Adionel Guimarães and
André Antônio dos Anjos

*Address all correspondence to: rausley@inatel.br, dayan@inatel.br, andre-anjos@inatel.br

National Institute of Telecommunications (Inatel), Santa Rita do Sapucaí – MG, Brazil

References

[1] FCC, ET Docket No 03-222 Notice of proposed rule making and order, December 2003.

[2] Mitola J, Maguire GQ. Cognitive radio: making software radios more personal. Personal Communications, IEEE. 1999;6(4):13-8.

[3] Ghasemi A, Sousa ES. Collaborative spectrum sensing for opportunistic access in fading environments. New Frontiers in Dynamic Spectrum Access Networks, 2005. DySPAN 2005. 2005 First IEEE International Symposium on. 2005. p. 131-6.

[4] Letaief KB, Zhang W. Cooperative Communications for Cognitive Radio Networks. Proceedings of the IEEE. 2009;97(5):878-93.

[5] IEEE Standard for Information Technology--Telecommunications and information exchange between systems Wireless Regional Area Networks (WRAN)--Specific requirements Part 22: Cognitive Wireless RAN Medium Access Control (MAC) and Physical Layer (PHY) Specifications: Policies and Procedures for Operation in the TV Bands. 2011.

[6] Akyildiz IF, Lo BF, Balakrishnan R. Cooperative spectrum sensing in cognitive radio networks: A survey. Elsevier Physical Communication. 4(1):40-62.

[7] Yates RD, Goodman D. Probability and Stochastic Processes: A Friendly Introduction for Electrical and Computer Engineers. 2nd ed. 2004.

[8] Sahai A, Hoven N, Tandra R. Some fundamental limits on cognitive radio. Allerton Conference on Control, Communications, and Computation. 2004. p. 1662-71.

[9] Digham FF, Alouini M-S, Simon MK. On the Energy Detection of Unknown Signals Over Fading Channels. Communications, IEEE Transactions on. 2007;55(1):21-4.

[10] Urkowitz H. Energy detection of unknown deterministic signals. Proceedings of the IEEE. 1967;55(4):523- 531.

[11] Cabric D, Mishra SM, Brodersen RW. Implementation issues in spectrum sensing for cognitive radios. Signals, Systems and Computers, 2004. Conference Record of the Thirty-Eighth Asilomar Conference on. 2004. p. 772- 776 Vol.1.

[12] Fehske A, Gaeddert J, Reed JH. A new approach to signal classification using spectral correlation and neural networks. New Frontiers in Dynamic Spectrum Access Networks, 2005. DySPAN 2005. 2005 First IEEE International Symposium on. 2005. p. 144-50.

[13] Zeng Y, Liang Y-C. Eigenvalue-based spectrum sensing algorithms for cognitive radio. Communications, IEEE Transactions on. 2009;57(6):1784-93.

[14] Kortun A, Ratnarajah T, Sellathurai M, Caijun Zhong, Papadias CB. On the Performance of Eigenvalue-Based Cooperative Spectrum Sensing for Cognitive Radio. Selected Topics in Signal Processing, IEEE Journal of. 2011;5(1):49-55.

[15] Nadler B, Penna F, Garello R. Performance of Eigenvalue-Based Signal Detectors with Known and Unknown Noise Level. Communications (ICC), 2011 IEEE International Conference on. 2011. p. 1-5.

[16] ITS Handbook [Internet]. Available from: http://road-network-operations.piarc.org/index.php?option=com_docman&task=cat_view&gid=93&Itemid=39&lang=en

[17] Nekovee M. Sensor networks on the road: the promises and challenges of vehicular ad hoc networks and vehicular grids. Workshop on Ubiquitous Computing and e-Research. Edinburgh, U.K; 2005.

[18] Blum JJ, Eskandarian A, Hoffman LJ. Challenges of intervehicle ad hoc networks. Intelligent Transportation Systems, IEEE Transactions on. 2004;5(4):347- 351.

[19] FCC. News Release, October 1999. Available from http://transition.fcc.gov/Bureaus/Engineering_Technology/News_Releases/1999/nret9006.html.

[20] Fawaz K, Ghandour A, Olleik M, Artail H. Improving reliability of safety applications in vehicle ad hoc networks through the implementation of a cognitive network. Telecommunications (ICT), 2010 IEEE 17th International Conference on. 2010. p. 798-805.

[21] Rawashdeh ZY, Mahmud SM. Communications in Vehicular Ad Hoc Networks, Mobile Ad-Hoc Networks: Applications, Xin Wang (Ed.), ISBN: 978-953-307-416-0, In-

Tech, 2011. Available from: http://www.intechopen.com/books/mobile-ad-hoc-networks-applications/communications-in-vehicular-ad-hoc-networks.

[22] Li H, Irick DK. Collaborative Spectrum Sensing in Cognitive Radio Vehicular Ad Hoc Networks: Belief Propagation on Highway. Vehicular Technology Conference (VTC 2010-Spring), 2010 IEEE 71st. 2010. p. 1-5.

[23] Lennett B. Rural broadband and the TV White space: How unlicensed access to vacante television channels can bring affordable wireless broadband to rural America. New America Foundation: Wireless Future Program, 2008.

[24] Mishra SM, Sahai A, Brodersen RW. Cooperative Sensing among Cognitive Radios. Communications, 2006. ICC '06. IEEE International Conference on. 2006. p. 1658-63.

[25] Wang XY, Ho P-H. A Novel Sensing Coordination Framework for CR-VANETs. Vehicular Technology, IEEE Transactions on. 2010;59(4):1936-48.

[26] Guimarães DA, Souza RAA, Barreto AN. Performance of Cooperative Eigenvalue Spectrum Sensing with a Realistic Receiver Model under Impulsive Noise. Accepted for publication in Journal of Sensor and Actuator Networks. 2012; Dec.

[27] Zeng Y, Liang Y-C. Covariance Based Signal Detections for Cognitive Radio. New Frontiers in Dynamic Spectrum Access Networks, 2007. DySPAN 2007. 2nd IEEE International Symposium on. 2007. p. 202-7.

[28] Guimarães DA, Souza RAA, Implementation-Oriented Model for Centralized Data-Fusion Cooperative Spectrum Sensing, Communications Letters, IEEE. 2012; 16(11), 1804-07. doi: 10.1109/LCOMM.2012.092112.121614.

[29] Cichocki A, Amari S. Adaptive Blind Signal and Image Processing. John Wiley and Sons, Inc.: Chichester, England, 2002.

[30] Mann I, McLaughlin S, Henkel W, Kirkby R, Kessler T. Impulse generation with appropriate amplitude, length, inter-arrival, and spectral characteristics. Selected Areas in Communications, IEEE Journal on. 2002;20(5):901-12.

[31] Lago-Fernández J, Salter J. Modeling Impulsive Interference in DVB-T: Statistical Analysis, Test Waveforms and Receiver Performance. BBC R&D white paper WHP 080, Apr. 2004.

[32] Middleton D. Non-Gaussian noise models in signal processing for telecommunications: new methods an results for class A and class B noise models. Information Theory, IEEE Transactions on. 1999;45(4):1129-49.

[33] Torio P, Sanchez MG. Generating Impulsive Noise [Wireless Corner]. Antennas and Propagation Magazine, IEEE. 2010;52(4):168-73.

[34] Torio P, Sanchez MG, Cuinas I. An algorithm to simulate impulsive noise. Software, Telecommunications and Computer Networks (SoftCOM), 2011 19th International Conference on. 2011. p. 1-4.

[35] Rasheed H, Rajatheva N. Spectrum Sensing for Cognitive Vehicular Networks over Composite Fading. International Journal of Vehicular Technology. 2011:1-9.

[36] Mecklenbrauker CF, Molisch AF, Karedal J, Tufvesson F, Paier A, Bernado L, et al. Vehicular Channel Characterization and Its Implications for Wireless System Design and Performance. Proceedings of the IEEE. 2011; 99(7):1189-212.

[37] Dhar S, Bera R, Giri RB, Anand S, Nath D, Kumar S. An Overview of V2V Communication Channel Modeling. IJCA Proceedings on International Symposium on Devices MEMS, Intelligent Systems & Communication (ISDMISC). 2011;24-34.